AMERICAN SOCIETY FOR MICROBIOLOGY | Infection and Immunity®

MICROBIAL IMMUNITY AND VACCINES

Construction and Characterization of the *Mycobacterium tuberculosis sigE fadD26* Unmarked Double Mutant as a Vaccine Candidate

Rogelio Hernandez-Pando,[a] Sung Jae Shin,[b] Simon Clark,[c] Stefano Casonato,[d] Martin Becerril-Zambrano,[a] Hongmin Kim,[b] Francesca Boldrin,[d] Dulce Mata-Espinoza,[a] Roberta Provvedi,[e] Ainhoa Arbues,[f]* Brenda Marquina-Castillo,[a] Laura Cioetto Mazzabò,[d] Jorge Barrios-Payan,[a] Carlos Martin,[f] Sang-Nae Cho,[b] Ann Williams,[c] Riccardo Manganelli[d]

[a]Experimental Pathology Section, Department of Pathology, National Institute of Medical Sciences and Nutrition Salvador Zubirán, Mexico City, Mexico

[b]Department of Microbiology, Institute for Immunology and Immunological Disease, Brain Korea 21 PLUS Project for Medical Science, Yonsei University College of Medicine, Seoul, South Korea

[c]Public Health England, Microbiology Services, Porton Down, Salisbury, Wiltshire, United Kingdom

[d]Department of Molecular Medicine, University of Padova, Padua, Italy

[e]Department of Biology, University of Padova, Padua, Italy

[f]Departamento de Microbiología, Facultad de Medicina, Universidad de Zaragoza, Zaragoza, Spain

Rogelio Hernandez-Pando, Sung Jae Shin, Simon Clark, and Stefano Casonato contributed equally to this work.

ABSTRACT Despite the great increase in the understanding of the biology and pathogenesis of *Mycobacterium tuberculosis* achieved by the scientific community in recent decades, tuberculosis (TB) still represents one of the major threats to global human health. The only available vaccine (*Mycobacterium bovis* BCG) protects children from disseminated forms of TB but does not effectively protect adults from the respiratory form of the disease, making the development of new and more-efficacious vaccines against the pulmonary forms of TB a major goal for the improvement of global health. Among the different strategies being developed to reach this goal is the construction of attenuated strains more efficacious and safer than BCG. We recently showed that a *sigE* mutant of *M. tuberculosis* was more attenuated and more efficacious than BCG in a mouse model of infection. In this paper, we describe the construction and characterization of an *M. tuberculosis sigE fadD26* unmarked double mutant fulfilling the criteria of the Geneva Consensus for entering human clinical trials. The data presented suggest that this mutant is even more attenuated and slightly more efficacious than the previous *sigE* mutant in different mouse models of infection and is equivalent to BCG in a guinea pig model of infection.

KEYWORDS tuberculosis, vaccine, BCG, sigma factor, SigE

Tuberculosis (TB) is a complex disease still considered one of the major threats to global human health. Even though it is a curable disease, its control poses a great challenge to the health care systems of countries with high TB incidence, due to the length of treatment, the difficulty of obtaining compliance, and the circulation of multidrug-resistant strains. The only available vaccine against TB, the attenuated strain of *Mycobacterium bovis* BCG, is effective in protecting children from disseminated forms of the disease but not in protecting adults from its pulmonary form; thus, it does not interrupt the *Mycobacterium tuberculosis* transmission chain (1). Recently, the scientific community has developed different vaccine candidates and vaccination strategies, approaching the challenge of developing a new vaccine against TB either as a prime vaccine that could replace BCG or as a booster for individuals previously vaccinated

Citation Hernandez-Pando R, Shin SJ, Clark S, Casonato S, Becerril-Zambrano M, Kim H, Boldrin F, Mata-Espinoza D, Provvedi R, Arbues A, Marquina-Castillo B, Cioetto Mazzabò L, Barrios-Payan J, Martin C, Cho S-N, Williams A, Manganelli R. 2020. Construction and characterization of the *Mycobacterium tuberculosis sigE fadD26* unmarked double mutant as a vaccine candidate. Infect Immun 88:e00496-19. https://doi.org/10.1128/IAI.00496-19.

Editor Sabine Ehrt, Weill Cornell Medical College

Address correspondence to Riccardo Manganelli, riccardo.manganelli@unipd.it.

* Present address: Ainhoa Arbues, Clinical Immunology Unit, Swiss Tropical and Public Health Institute, Basel, Switzerland.

Received 28 June 2019
Returned for modification 27 July 2019
Accepted 30 September 2019

Accepted manuscript posted online 7 October 2019
Published 17 December 2019

with BCG (2). A leading strategy is focused on the development of attenuated mycobacterial strains that are more efficient in eliciting protective immunity than BCG (3, 4). To achieve this goal, different approaches have been used, including the construction of recombinant strains of BCG that can express additional protective antigens not encoded in its genome (5–7) or that can evade the phagosome, thus facilitating antigen presentation (8), and the use of attenuated *M. tuberculosis* strains, which inherently express a broader repertoire of mycobacterial antigens (9, 10).

Previously, we showed that an *M. tuberculosis sigE*-null mutant was strongly attenuated and conferred better protection from aerosol infection with *M. tuberculosis* than BCG in both mice and guinea pigs (11, 12). SigE, one of ten extracytoplasmic function (ECF) sigma factors encoded in the *M. tuberculosis* genome (13), is subject to very complex regulation (14, 15). It has been shown to be involved in setting the basal level of sensitivity to several TB drugs (16) and in the development of persisters that are able to escape drug bactericidal activity (16), and it is essential for virulence in macrophages (17), mice (18), and guinea pigs (12). The precise mechanism behind these phenotypes is still not known, but the failure to maintain surface homeostasis and possibly remodeling of its surface composition in response to surface stress might play important roles (13, 17, 19). Moreover, SigE has been shown to be required for blocking phagosome maturation, thus leading to more-efficient antigen presentation (20).

To begin the development of a new mutant that fulfills the Geneva Consensus requirements for entering human clinical trials (21, 22), we recently constructed a new *M. tuberculosis sigE*-null mutant, designated ST218, in which the entire copy of the gene was deleted and which lacked any resistant marker (20). In this article, we describe a further evolution of this strain, into which we introduced a second unmarked mutation by deleting *fadD26*, a gene essential for virulence, whose product is involved in the biosynthesis of phthiocerol dimycocerosates (23). This new TB vaccine candidate was shown to be more attenuated and more protective than BCG; thus, it is a promising new prime TB vaccine candidate in the pipeline.

RESULTS

Construction of a double unmarked *sigE fadD26* mutant in *M. tuberculosis*. Using a two-step procedure based on the suicide plasmid pAZ5 (9), the *fadD26* gene was replaced by a Hyg cassette flanked by *res* sites in the unmarked *sigE*-null mutant ST218 (see Fig. S1 in the supplemental material) (20). The Hyg cassette was then removed to produce a double unmarked *sigE fadD26* mutant that was named TB223 (see Materials and Methods).

The *sigE fadD26* double mutant TB223 is more attenuated than BCG. One of the requirements of the Geneva Consensus for an *M. tuberculosis* mutant to enter clinical trials is that its attenuation must be comparable to that of BCG in relevant animal models. To prove that TB223 fulfills this criterion, its virulence was compared with that of BCG in SCID and nude mice. For this purpose, groups of 20 mice were infected by subcutaneous inoculation at the base of the tail with one dose of 8,000 CFU of BCG or TB223. Only 10% of the BCG-infected SCID mice were still alive after 5 weeks of infection, compared to 90% of TB223-infected mice, but the survival of the latter was reduced to only 10% after 9 additional weeks, suggesting greater sensitivity of TB223 than of BCG to innate immunity (Fig. 1A). In nude mice, the picture was slightly different: TB223-infected mice survived until the 10th week of infection, after which their survival started to decrease gradually. However, the survival of BCG-infected mice decreased very rapidly starting from the 15th week of infection, and none of these mice survived to week 19, when 60% of TB223-infected mice were still alive (Fig. 1B).

Comparison of the attenuation of the *sigE fadD26* double mutant TB223 and the *sigE* single mutant TB218. The virulence of the new double mutant was compared with that of the *sigE* single mutant TB218 in BALB/c mice infected with a high bacterial dose (2.5×10^5 CFU) by the intratracheal route. As shown in Fig. 2A, none of the mice infected with wild-type (WT) H37Rv and 30% of the mice infected with TB218 were still alive after 17 weeks of infection. However, the survival rate of the mice infected with

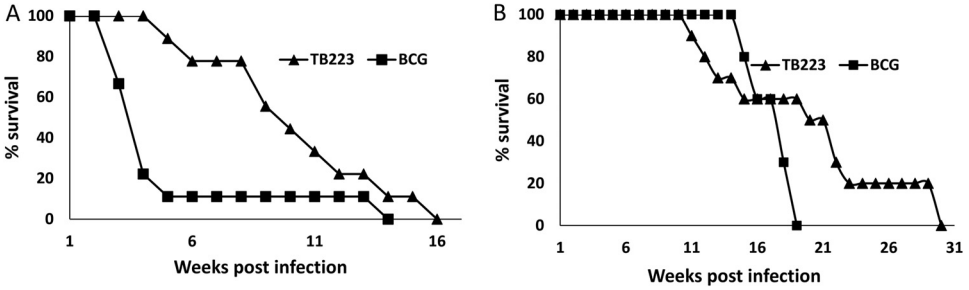

FIG 1 Survival of SCID (A) or nude (B) mice (20 mice per strain) infected by the subcutaneous route in the base of the tail (8,000 CFU) with *M. tuberculosis* TB223 or BCG. Survival curves were obtained by plotting the number of surviving mice as a function of time using the Kaplan-Meier algorithm. The curves in panel A were statistically different from each other ($P < 0.0009$).

the new double mutant at the same time point was 70%. Figure 2B shows the lung bacterial burdens during the same experiment: after 21 days of infection, the numbers of bacteria in the different groups were similar. However, after 60 days of infection, the bacterial burdens detected in the lungs of mice infected with the WT strain showed a

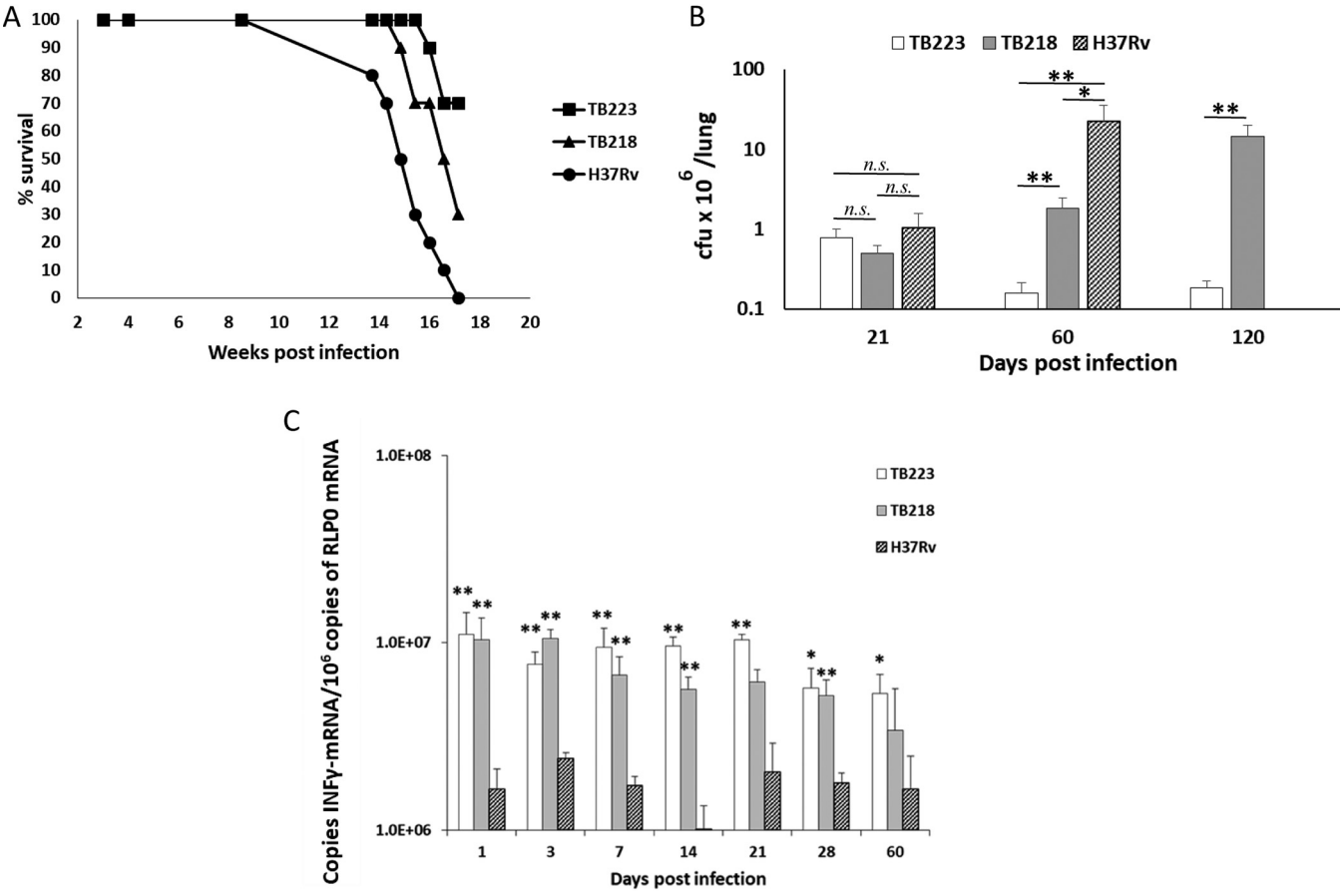

FIG 2 Comparisons of survival and bacillary loads for BALB/c mice infected intratracheally with different mycobacterial strains: the *sigE* mutant TB218, the *sigE fadD26* double mutant TB223, and the parental strain H37Rv. (A) Survival curve constructed with 20 mice per strain. Kill curves were obtained by plotting the number of dying mice as a function of time using the Kaplan-Meier algorithm. The survival of mice infected with the two different mutants did not differ statistically. However, the survival of mice infected with wild-type H37Rv was different from that of mice infected with either of the two mutants (P, <0.0001 for H37Rv versus TB223 and <0.0095 for H37Rv versus TB218). (B) Bacterial burdens in the lungs. Mice were sacrificed at the indicated days after infection, and lungs (n, 4 per group per time point) were used for the determination of CFU. At the later time points, mice infected with the double mutant TB223 showed significantly lower bacillary loads than the other groups. Asterisks indicate statistical significance (*, $P < 0.05$; **, $P < 0.01$). n.s., not significant. (C) Quantitative expression of IFN-γ mRNA in lungs from mice infected with H37Rv, TB218, or TB223 was determined by real-time PCR. Data are means and standard deviations of results from four different animals at each time point. Asterisks indicate statistical significance for comparisons with H37Rv-infected mice (*, $P < 0.05$; **, $P < 0.01$).

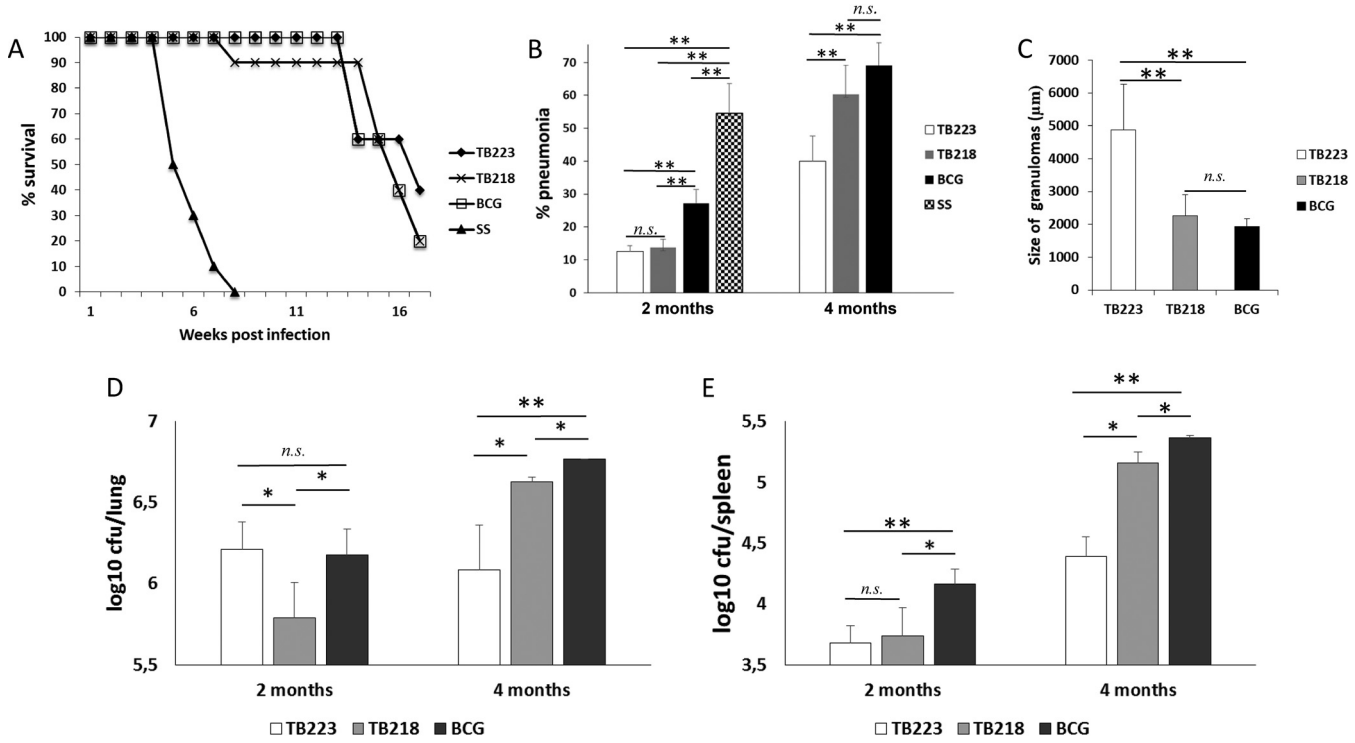

FIG 3 Survival, lung and spleen bacillary loads, and results of automated morphometry after intratracheal challenge with the highly virulent *M. tuberculosis* Harlem genotype 5186 for BALB/c mice vaccinated with TB218, TB223, or BCG and for nonvaccinated control animals (SS). (A) Survival of the different groups of BALB/c mice (20 mice per strain) vaccinated with the indicated strains. Survival curves were obtained by plotting the number of surviving mice as a function of time using the Kaplan-Meier algorithm. The survival of vaccinated mice was statistically different from that of unvaccinated mice ($P < 0.0001$), while the survival of the animals vaccinated with the three different vaccines was not significantly different. (B) Percentage of the lung surface affected by pneumonia, determined by automated morphometry. (C) Sizes of granulomas, measured by automated morphometry. (D and E) Bacillary loads in the lungs (D) and spleens (E) of the different groups of BALB/c mice vaccinated with the indicated strains after 60 and 120 days postchallenge. The results are expressed as means ± standard deviations for four mice. Asterisks indicate statistical significance (*, $P < 0.05$; **, $P < 0.01$) for differences between groups. No data are presented for the nonvaccinated control animals at 2 and 4 months postchallenge, since no surviving animals were available.

marked increase over those with the two mutant strains. After 120 days of infection, mice infected with the *sigE* single mutant also showed a marked increase in lung bacterial burdens, while those infected with the new double mutant were still able to control the infection, suggesting a higher attenuation of the double mutant than of the single mutant. It is worth noting that both *sigE* mutants were able to induce higher levels of gamma interferon (IFN-γ) expression in the lungs of infected mice than their parental strain H37Rv (Fig. 2C).

Comparative protection against *M. tuberculosis* in BALB/c mice vaccinated with the *sigE* mutant TB218, the *sigE fadD26* mutant TB223, or BCG. To compare the levels of protection induced by BCG and the *sigE* mutants, groups of BALB/c mice (40 per group in 2 separate experiments) were vaccinated by subcutaneous inoculation at the base of the tail with 8,000 CFU of the respective strain. At 60 days postvaccination, mice were challenged intratracheally with 2.5×10^5 CFU of *M. tuberculosis* 5186. The survival curves of the animals after infection, shown in Fig. 3A, clearly indicate that the three strains protected the animals from death at comparable levels. However, when we evaluated the bacterial burdens in the lungs and spleens of infected animals at 60 and 120 days postinfection (Fig. 3D and E), it was clear that the double mutant protected better than the single mutant and BCG in both the lung and the spleen. Areas of pneumonia in the lungs of infected mice were also measured, and mice vaccinated with the double mutant showed less TB-associated pathology than those vaccinated with the single mutant TB218 or with BCG (Fig. 3B; see also Fig. S2A in the supplemental material). Finally, analysis of the sizes of granulomas in infected lungs showed that mice vaccinated with the double mutant TB223 had larger granulomas

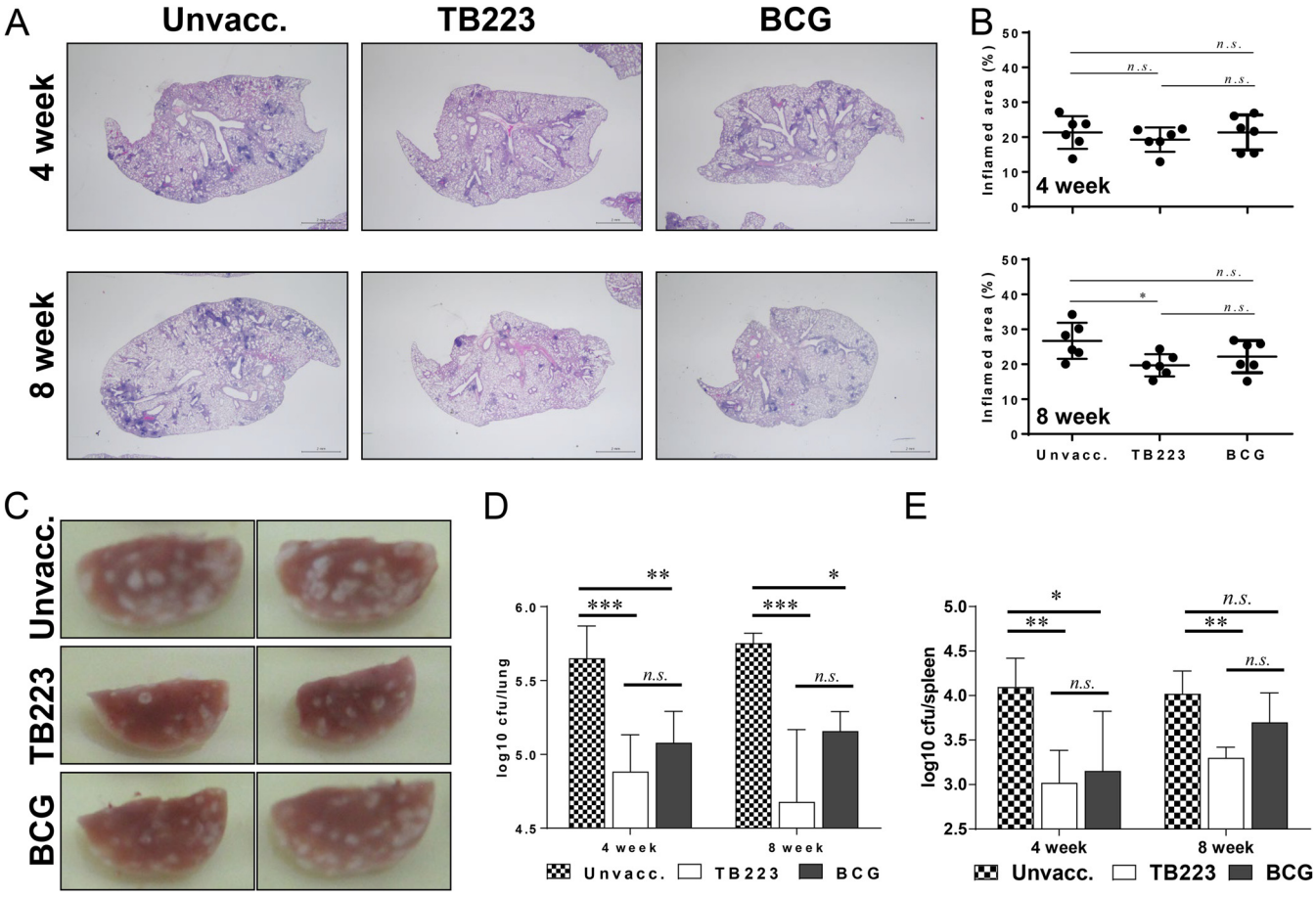

FIG 4 Protective efficacy of BCG and TB223 immunization against infection with *M. tuberculosis* Beijing strain K. (A) H&E-stained sections (*n*, 6 mice/group) of lungs from nonimmunized (Unvacc.), BCG-immunized, and TB223-immunized mice at 4 and 8 weeks after challenge with aerosolized *M. tuberculosis* Beijing strain K (full-size images; bars, 2 mm). (B) Areas of lung inflammation, calculated using the ImageJ program (National Institutes of Health, USA). (C) Gross pathology of lungs from nonimmunized, BCG-immunized, and TB223-immunized mice at 8 weeks after challenge. (D and E) Bacterial burdens in the lungs (D) and spleens (E) of nonimmunized, BCG-immunized, and TB223-immunized mice at 4 and 8 weeks after infection with *M. tuberculosis* Beijing strain K. Data are means and standard deviations of results for six mice. Asterisks indicate statistical significance (*, $P < 0.05$; **, $P < 0.01$; ***, $P < 0.001$) for comparison with mice infected with *M. tuberculosis* Beijing strain K.

after 120 days postinfection (Fig. 3C; also Fig. S2B). In this murine model, granuloma size correlates with protection (24), so the larger granulomas confirmed the improved protection conferred by the double mutant TB223.

Comparative protection against *M. tuberculosis* in C57BL/6 mice vaccinated with the *sigE fadD26* mutant TB223 or BCG. Protection was also evaluated in a Beijing challenge model. To compare the levels of protection induced by BCG and the *sigE fadD26* mutant, groups of C57BL/6 mice were vaccinated subcutaneously. Six weeks after immunization, mice were challenged with 200 CFU of *M. tuberculosis* Beijing strain K via the aerosol route. After 4 and 8 weeks postinfection, mice were sacrificed. TB223-immunized mice showed lower levels of pathology (inflammation) than nonimmunized or BCG-immunized mice, especially at 8 weeks postinfection (Fig. 4A and B). In gross pathology analysis, TB223 immunization showed the most effective protection at 8 weeks postinfection (Fig. 4C). These protective efficacies correlated with bacterial burdens. TB223-vaccinated mice had significantly lower bacterial burdens than the nonvaccinated control group and lower bacterial burdens than BCG-vaccinated mice in both the lung and the spleen, although the latter difference did not reach statistical significance (Fig. 4D and E), suggesting that TB223 has greater efficacy than BCG in the C57BL/6 mouse model of infection with *M. tuberculosis* Beijing strain K.

Comparative protection against *M. tuberculosis* in guinea pigs vaccinated with the *sigE fadD26* mutant or BCG. Finally, the protective potential of the TB223 strain

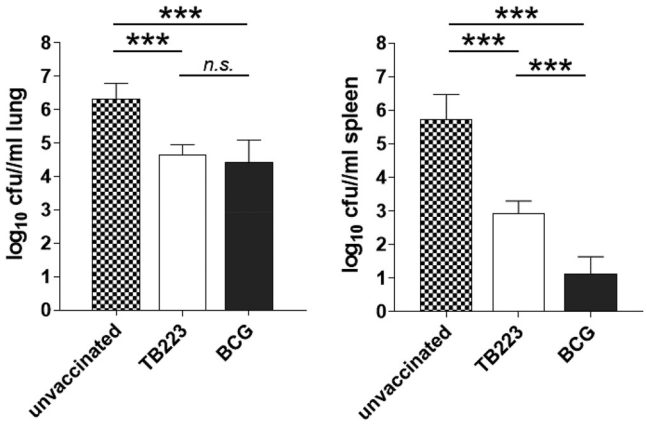

FIG 5 Bacillary loads in the lungs (left) and spleens (right) of guinea pigs vaccinated with TB223 or BCG Danish 1331, or in those of unvaccinated control animals, 4 weeks after aerosol challenge with *M. tuberculosis* H37Rv. Animals were vaccinated once subcutaneously with 5×10^4 CFU in 250 μl and were challenged 12 weeks postvaccination. Bacterial load data are expressed as $\log_{10}$ total CFU. Bars, group means ($n = 8$); error bars, standard errors of the means. Asterisks indicate statistical significance (***, $P < 0.001$; *n.s.*, not significant [$P > 0.05$]) in comparison to either BCG-vaccinated or unvaccinated guinea pigs.

was compared to that of BCG in an established short-term (4-week) guinea pig infection model. Animals were vaccinated once with 5×10^4 CFU by the subcutaneous route of delivery and were infected with *M. tuberculosis* at week 12. As shown in Fig. 5, the level of protection (as measured by the bacterial load) induced by TB223 in the lungs was equivalent to that obtained with BCG ($P = 0.4$), although TB223 was less protective than BCG in the spleen ($P < 0.001$).

DISCUSSION

In previous work, we demonstrated that an *M. tuberculosis* mutant missing the gene encoding the alternative sigma factor SigE (ST28), beyond being severely attenuated, induced strong IFN-γ and tumor necrosis factor alpha (TNF-α) responses (11). When this mutant was used to vaccinate mice or guinea pigs before challenge with virulent *M. tuberculosis*, it was able to induce better protection than BCG (11, 12). In the original mutant (ST28), *sigE* was disrupted by a cassette conferring hygromycin resistance, ruling out the use of this construct in clinical trials. For this reason, we recently constructed a new, unmarked *sigE* mutant in which the entire *sigE* gene was deleted (20). To further improve the biosafety of this strain and to fulfill the Geneva Consensus for entering clinical trials (21, 22), we introduced a second unmarked mutation, deleting *fadD26*, into this strain. The deletion of this gene, whose product is required for the biosynthesis of phthiocerol dimycocerosates and is essential for virulence, has already been used successfully to improve the biosafety, without decreasing the protective potential, of another candidate vaccine: the *phoP fadD26* mutant MTBVAC, the first attenuated *M. tuberculosis* mutant to be tested in clinical trials (9).

Despite its good safety profile, BCG vaccination can cause disseminated disease in severely immunocompromised children (25), so one of the essential characteristics of a new attenuated vaccine is a better attenuation profile (3, 7). In this study, we used different mouse infection models to characterize the virulence of the *sigE fadD26* double mutant and to compare it to those of the *sigE* single mutant and BCG.

First, we showed that the double mutant was more attenuated than BCG in both nude and SCID mice (Fig. 1). Attenuation was more pronounced in SCID mice than in nude mice. While SCID mice suffer severe humoral and cellular immunodeficiency, humoral immunity is not affected in nude mice. Consequently, it is possible that nude mice have sufficient antibody production, which can contribute to bacterial killing facilitated by an antibody-mediated mechanism. Then we also demonstrated that the

double mutant reached lower bacillary loads in the lungs of immunocompetent mice than the *sigE* single mutant, suggesting higher attenuation for the former (Fig. 2).

The protection elicited by the double mutant was then characterized in two different murine models and one guinea pig model of infection. In a previous report, we showed that mice vaccinated with the single *sigE* mutant were more protected against *M. tuberculosis* infection than mice vaccinated with BCG. Interestingly, the difference from BCG was more evident when mice were challenged with a hypervirulent strain of *M. tuberculosis* (11). For this reason, in the experiments described in this paper, mice were challenged with highly virulent clinical strains and not with H37Rv. In the first model, BALB/c mice vaccinated with either the *sigE fadD26* double mutant or the *sigE* single mutant were then challenged by intratracheal infection with *M. tuberculosis* Harlem 5186 (26, 27). After 2 months postinfection, only mice vaccinated with the single mutant showed lung bacillary loads lower than those in BCG-vaccinated mice, while animals vaccinated with either the double or the single mutant showed decreased bacillary loads in their spleens. Interestingly, mice vaccinated with the double mutant showed less lung pathology than BCG-vaccinated mice, even when the lung bacillary loads of the animals belonging to the two groups were comparable. After two additional months, the number of bacteria in the lungs of mice vaccinated with the double mutant remained stable, while that in the lungs of mice vaccinated with the single mutant or BCG increased to reach values statistically higher than those found in the animals vaccinated with the double mutant. This finding suggested that the double mutant conferred a more potent and longer-lasting protection than the other two strains. Reduced bacterial loads correlated with improved survival rates. The groups of animals vaccinated with BCG or the single mutant had equivalent survival rates, while mice vaccinated with the double mutant had an improved survival rate, significantly reduced TB-associated pathology, and larger granulomas. The observed increase in efficacy correlated with relatively higher IFN-γ expression in BALB/c mice infected with a high dose of the double mutant delivered by the intratracheal route.

In the second model, C57BL/6 mice were vaccinated either with the double mutant or with BCG and were then challenged by the aerosol route with *M. tuberculosis* Lineage 2 Beijing strain K (28). In this case also, the double mutant was shown to induce slightly better protection than BCG, suggesting that this vaccine candidate has potential utility in East Asian countries, where the Beijing genotype is predominant in those vaccinated with BCG.

In the guinea pig model, the *sigE fadD26* double mutant of *M. tuberculosis* demonstrated both safety and efficacy against aerosol challenge with *M. tuberculosis* H37Rv. This vaccine gave protection equivalent to that of BCG in the lungs and may offer advantages over BCG, such as the provision of a broader repertoire of protective antigens and the generation of more *M. tuberculosis*-like responses without disease. More studies are required in order to further understand the immune responses in guinea pigs and to determine if this vaccine could be more efficacious in a revaccination regimen.

Live attenuated vaccines based on rational attenuation of *M. tuberculosis* are showing promise in the preclinical space, and such candidates are currently in clinical trials (e.g., MTBVAC). Here, we report an evaluation of the safety and protective efficacy of a *sigE fadD26* double mutant of *M. tuberculosis*. These results suggest that the *sigE fadD26* mutant of *M. tuberculosis* could be used as an effective vaccine to replace or supplement BCG in infants or adults with historic BCG vaccination who live in countries where TB is endemic.

MATERIALS AND METHODS

Bacterial strains, growth media, and transformation conditions. The following bacterial strains were used: *Escherichia coli* K-12 mc1061 (29) and *E. coli* XL1-Blue, *M. tuberculosis* TB218 (20), BCG Phipps (30), BCG Pasteur (30), BCG Danish 1331 (31), *M. tuberculosis* Harlem 5186 (26, 27), and *M. tuberculosis* Beijing K (28) (see Table S1 in the supplemental material). *E. coli* strains were grown at 37°C in Luria-Bertani (LB) broth or on LB agar plates. Mycobacterial strains were grown at 37°C in Middlebrook 7H9 broth (Becton Dickinson [BD]) in 150-ml roller bottles with slow rotation (3 rpm) or on 7H10 agar

plates (BD), supplemented with 0.2% glycerol and 0.05% Tween 80. For the growth of *M. tuberculosis*, the medium was supplemented with 10% albumin, dextrose, and NaCl (ADN). When required, antibiotics or sucrose were added to the medium at the following concentrations: kanamycin (Km), 50 μg/ml; hygromycin (Hyg), 150 mg/ml (*E. coli*) or 50 mg/ml (*M. tuberculosis*); sucrose (Suc), 2% (wt/vol).

Construction of an unmarked *sigE fadD26* double mutant of *M. tuberculosis*. TB218 (20) was electroporated with pAZ5 (9). Transformants were selected on Hyg-containing plates, and single colonies were assayed for Suc sensitivity in order to select strains with the plasmid integrated by insertional duplication (TB218::pAZ5). In the second step, 10 Hyg^r Suc^s colonies (TB218::pAZ5 1 to TB218::pAZ5 10) were propagated in liquid medium to allow the second recombination event to occur, and serial dilutions were plated onto Suc-containing plates to select bacteria that had lost the *sacB* gene. Hyg^r Suc^r clones were tested by PCR using two primers (RP1248 and RP1249) (Table S1 in the supplemental material) internal to the *fadD26* gene (Fig. S1A). As shown in Fig. S1B, no PCR product was amplified from 4 of the 10 clones tested, suggesting correct deletion of *fadD26*. These clones were further tested using two different pairs of primers (RP1244–RP1245 [primer pair A] and RP1246–RP1247 [primer pair B]) (Table S1) hybridizing in the *res* sites or outside the *fadD26*-flanking regions cloned into pAZ5 (9) (Fig. S1A). In the presence of a correct deletion of *fadD26*, we would expect to obtain a PCR product of 905 bp from primer pair A and a band of 1,532 bp from primer pair B. As shown in Fig. S1C, all the strains gave PCR products of the correct sizes, confirming the correct deletion of *fadD26* in these strains. One of these clones (clone 2.1) was named TB219 and was conserved for further studies.

Finally, plasmid pAZ20 (9) was introduced into TB219 to generate the unmarked *fadD26* mutant. pAZ20 expresses the *tnpR* gene under the control of promoter P_{blaF^*} and includes the *sacB* gene, which provides negative selection for the spontaneous loss of the helper plasmid when plated on a Suc-containing medium. Transformants were selected on Km-containing plates, grown until saturation in liquid medium, and plated onto Suc-supplemented plates. The clones obtained were tested by PCR using primers RP1244 and RP1246 (Table S1 and Fig. S1A in the supplemental material). In the presence of a correct deletion of *fadD26*, we would expect to obtain a PCR product of 2,633 bp, while no deletion would result in an expected PCR product of 4,004 bp. As shown in Fig. S1D, a product of the correct size was amplified from a clone (named TB223). The correct sequence of the fragment was finally confirmed by Sanger sequencing (not shown).

Mouse infection and RNA extraction from lung homogenates. Male BALB/c mice, 8 to 10 weeks old, were used to evaluate the virulence of strains by the determination of survival, pulmonary bacterial loads, and TB pathology (pneumonia and granuloma size), and the immune response was evaluated by measurement of the expression of gamma interferon (IFN-γ), as described previously (1). Briefly, bacilli were grown in Middlebrook 7H9 liquid culture medium and were monitored by densitometry. As soon as the culture reached mid-log phase, the bacilli were harvested and were suspended in phosphate-buffered saline (PBS) containing 0.05% Tween 80 by shaking for 10 min with glass beads. Large clumps of bacilli were removed from the suspension by centrifugation for 1 min at 350 $\times$ *g*. Then a preliminary bacterial count was achieved by smearing the supernatant at a known ratio of volume to area and counting 10 random fields after Ziehl-Neelsen staining. The suspension was finally diluted to 2.5×10^5 CFU in 100 μl of PBS and was aliquoted at −70°C. Before use, bacteria were recounted, and viability was checked as described previously (22). To induce progressive pulmonary TB, mice were anesthetized with sevoflurane and were inoculated intratracheally with 2.5×10^5 CFU of either *M. tuberculosis* H37Rv, the *sigE* mutant (TB218), or the *sigE fadD26* double mutant (TB223) suspended in 100 μl PBS (15). After animal infection, the remnant of the bacterial inoculum was plated onto solid agar to confirm the number of CFU administered to the animals. Infected mice were kept in a vertical position until the effect of the anesthesia had passed. Animals were maintained in groups of five in cages fitted with microisolators under negative pressure. Ten mice from each group were left undisturbed so as to allow survival to be recorded from day 8 up to week 32 after infection. Six animals from each group were sacrificed by exsanguination at 21, 60, and 120 days after infection. Both lung lobes were snap-frozen in liquid nitrogen and were then stored at −70°C for microbiological and immunological analysis (15). All procedures were performed in a laminar flow cabinet in a biosafety level 3 facility. Two independent experiments were performed.

To confirm the attenuation of the *sigE* mutants, groups of 10 SCID and nude mice were infected subcutaneously at the base of the tail with one dose of 8,000 CFU of the live *sigE* mutant, double mutant, or BCG substrain Phipps, and the survival of these mice was recorded. After animal infection, the remnant of the bacterial inoculum was plated onto agar to confirm the number of CFU administered to the animals (1).

Determination of CFU counts in infected lungs. Right lungs from four mice at each time point, in two separate experiments, were used to determine bacterial burdens by colony counts on solid agar. Lungs were homogenized with a Polytron homogenizer (Kinematica, Lucerne, Switzerland) in sterile 50-ml tubes containing 3 ml of isotonic saline. Four dilutions of each homogenate were spread onto duplicate plates containing Bacto Middlebrook 7H10 agar (Difco Labs, Detroit, MI) enriched with oleic acid-albumin-dextrose-catalase (OADC). Plates were incubated for 21 days prior to determination of CFU counts (1).

Evaluation of protection of vaccinated BALB/c mice against infection with virulent *M. tuberculosis* Harlem 5186. Groups of 8-week-old BALB/c mice were vaccinated subcutaneously at the base of the tail with 8,000 live bacilli of BCG substrain Phipps, the *sigE* mutant, or the *sigE fadD26* double mutant. At 60 days postvaccination, mice were challenged by the intratracheal route with 2.5×10^5 CFU of the hypervirulent Harlem strain code 5186. This is a clinical strain collected from an epidemiological study in the south of Mexico; it is highly virulent and transmissible in the community and in this murine model

(26). The control group consisted of unvaccinated mice intratracheally infected with the same dose of strain 5186. After 2 and 4 months postchallenge, protection was determined by the quantification of bacterial CFU in lung and spleen homogenates and by automated morphometry, measuring TB pathology in the lung affected by pneumonia and granuloma size. Ten further animals per group remained in the study, were monitored until they reached a humane endpoint, and were then sacrificed. Deaths were recorded in order to construct survival curves using the Kaplan-Meier algorithm (32). Two independent experiments were performed.

Preparation of lung tissue for histology and automated morphometry. For histology and automated morphometry, the left lobe of the lung was fixed by intratracheal perfusion with 4% formaldehyde for 24 h and was then sectioned through the hilus and embedded in paraffin. Sections (thickness, 5 μm) were stained with hematoxylin and eosin (H&E) for the histological-morphometric analysis. The percentage of the pulmonary area affected by pneumonia and the sizes (expressed as areas in square micrometers) of granulomas were determined using an automated image analyzer (Leica QWin; Leica, Milton Keynes, United Kingdom) (1). Granulomas are well-limited nodules constituted by lymphocytes and macrophages. From each lung, three serial sections, 100 μm apart, were obtained. In each section, all the granulomas were measured, and their areas in square micrometers were determined. To determine the extent of pneumonia, each slide was photographed using a camera system that obtained an image of the full lung area, corresponding to an area of 100%. Then the pneumonic areas were delimited and measured with the software analyzer. Finally, the percentage of the lung surface area affected by pneumonia was determined. Measurements were done blind, and the data are reported as mean values $\pm$ standard deviations (SD) from three different mice per group in two independent experiments.

RT-PCR analyses. Left or right lung lobes from three different mice per group in two different experiments were used to isolate mRNA using the RNeasy minikit (Qiagen) according to the recommendations of the manufacturer. The quality and quantity of RNA were evaluated through spectrophotometry (260/280 nm) and on agarose gels. Reverse transcription of the mRNA was performed using 5 μg RNA, oligo(dT), and the Omniscript kit (Qiagen, Inc.). Real-time PCR (RT-PCR) was carried out using the 7500 real-time PCR system (Applied Biosystems) and the QuantiTect SYBR green master mix kit (Qiagen).

Standard curves of the quantified and diluted PCR product, as well as negative controls, were included in each PCR run. Specific primers for genes encoding acidic ribosomal protein (RLP0) as a housekeeping gene (forward [FWD], 5′-CTCTCGCTTTCTGGAGGGTG-3′; reverse [RV], 5′-ACGCGCTTGTAC CCATTGAT-3′) and IFN-γ (FWD, 5′-GGTGACATGAAAATCCTGCAG-3′; RV, 5′-CCTCAAACTTGGCAATACTCA TGA-3′) were designed using the Primer Express program (Applied Biosystems). The cycling conditions used were as follows: initial denaturation at 95°C for 15 min, followed by 40 cycles at 95°C for 20 s, 60°C for 20 s, and 72°C for 34 s. Quantities of the specific mRNA in the sample were measured according to the corresponding gene-specific standard. The mRNA encoding RLP0 was used as an internal invariant control to normalize the expression of the IFN-γ gene. Data are shown as copies of cytokine-specific mRNA per 10^6 copies of RLP0-specific mRNA (1).

Evaluation of protection against infection with *M. tuberculosis* Beijing strain K in vaccinated C57BL/6 mice. *M. tuberculosis* strain K (28) was obtained from the strain collections at the Korean Institute of Tuberculosis (KIT; Osong, Chungcheongbuk-do, South Korea). BCG (Pasteur 1173P2) was kindly provided by the Pasteur Institute (Paris, France). C57BL/6 mice were immunized subcutaneously with BCG (1.0×10^5 CFU/mouse) or TB223 (2.0×10^5 CFU/mouse). Six weeks after the final immunization, mice were exposed to *M. tuberculosis* K for 60 min in the inhalation chamber of an airborne infection apparatus calibrated to deliver a predetermined dose (Glas-Col, Terre Haute, IN). To confirm the initial bacterial burden, four mice were euthanized 1 day later, and lung homogenates were plated to confirm that approximately 200 viable bacteria were delivered to the lungs of each mouse. After 4 and 8 weeks postchallenge, levels of protection were determined by the quantification of bacterial CFU in lung and spleen homogenates. For histology analyses, the left lung lobes were fixed by intratracheal perfusion with 4% formaldehyde for 24 h and were embedded in paraffin. Lung lobes were sectioned (thickness, 4 μm) and were stained with hematoxylin and eosin for the histological-morphometric analysis.

Vaccination and infection of guinea pigs. Guinea pigs (Dunkin-Hartley strain) free from pathogen-specific infection, with a body weight of 250 to 350 g, were randomly assigned to vaccine groups. Groups of eight guinea pigs were vaccinated once on the nape, by the subcutaneous route, with 5×10^4 CFU of either the *M. tuberculosis sigE fadD26* mutant or BCG Danish 1331 (as a positive control). Eight animals remained unvaccinated as a negative-control group.

Twelve weeks after vaccination, all animals were challenged by the aerosol route with *M. tuberculosis* strain H37Rv, grown in batch culture under defined conditions (33). Challenge was performed using a contained Henderson apparatus in conjunction with an AeroMP control unit as described previously (34–36). The challenge suspension was adjusted to deliver an estimated retained, inhaled low dose of approximately 10 to 20 CFU to the lungs of each animal (37). The suspension of *M. tuberculosis* in the nebulizer was plated onto Middlebrook 7H11 OADC selective agar in order to measure the concentration and confirm retrospectively that the expected dose had been delivered.

Measurement of protection in guinea pigs. Protection was determined by measuring the bacterial burden 4 weeks after challenge, when guinea pigs were killed by an overdose of intraperitoneally delivered sodium pentobarbital. At necropsy, lungs and spleens were removed as described previously (10). For bacterial load analysis, each tissue was homogenized in 2 ml of sterile PBS. Each tissue homogenate was serially diluted in sterile PBS, and 100 μl of each dilution was plated in duplicate onto Middlebrook 7H11 OADC selective agar. Plates were incubated at 37°C for as long as 4 weeks. After

incubation, colonies were enumerated (as CFU), and the concentration of bacilli per milliliter of each sample was calculated. Bacterial load data are expressed as $\log_{10}$ CFU per milliliter.

Efficacy was determined by pairwise comparisons between each vaccine group and the control group, and differences were considered statistically significant if the *P* value was <0.05. The bacterial load in each group was compared using a two-sample *t* test.

Ethics statements. Animal studies with Beijing strain K-infected C57BL/6 mice were carried out in accordance with the guidelines of the Korean Food and Drug Administration (KFDA; Osong, South Korea). The experimental protocols were reviewed and approved by the Ethics Committee and Institutional Animal Care and Use Committee (permit no. 2013-0145) of the Laboratory Animal Research Center at Yonsei University College of Medicine (Seoul, South Korea). All other studies with mice were approved by the Institutional Ethics Committee of the National Institute of Medical Sciences and Nutrition Salvador Zubiran in accordance with the guidelines of the Mexican national regulations on Animal Care and Experimentation (NOM 062-ZOO-1999; permit code PAT-973-13/15-1).

The guinea pig study was conducted according to the United Kingdom Home Office Legislation for animal experimentation and was approved by a local ethics committee at Public Health England (Porton Down, United Kingdom) (license no. 30-3236). Each animal was identified using subcutaneously implanted microchips (Plexx, the Netherlands) to enable blinding of the analyses wherever possible. Group sizes were determined by statistical power calculations (Minitab, version 16) performed using previous data (SD, approximately 0.5) to detect a 1.0-$\log_{10}$ difference in the median number of CFU per milliliter.

SUPPLEMENTAL MATERIAL

Supplemental material is available online only.

SUPPLEMENTAL FILE 1, PDF file, 3.7 MB.

ACKNOWLEDGMENTS

This work was supported by the European Community Seventh Framework Program (FP7/2007-2013) under grant agreement 241745 and by the Science and Technology Institute of Mexico City (grant agreement PICSA12-173). Experiments performed in the United Kingdom were supported by the Department of Health, United Kingdom. The views expressed in this publication are those of the authors and not necessarily those of the Department of Health.

We thank the staff of the Biological Investigations Group at PHE Porton for assistance in conducting studies and Faye Lanni for aerobiology and bacteriology support.

REFERENCES

1. Porcelli SA, Jacobs WR, Jr. 2019. Exacting Edward Jenner's revenge: the quest for a new tuberculosis vaccine. Sci Transl Med 11:eaax4219. https://doi.org/10.1126/scitranslmed.aax4219.
2. Delogu G, Manganelli R, Brennan MJ. 2014. Critical research concepts in tuberculosis vaccine development. Clin Microbiol Infect 20(Suppl 5):59–65. https://doi.org/10.1111/1469-0691.12460.
3. Soundarya JSV, Ranganathan UD, Tripathy SP. 2019. Current trends in tuberculosis vaccine. Med J Armed Forces India 75:18–24. https://doi.org/10.1016/j.mjafi.2018.12.013.
4. Ernst JD. 2018. Mechanisms of M. tuberculosis immune evasion as challenges to TB vaccine design. Cell Host Microbe 24:34–42. https://doi.org/10.1016/j.chom.2018.06.004.
5. Sali M, Di Sante G, Cascioferro A, Zumbo A, Nicolo C, Dona V, Rocca S, Procoli A, Morandi M, Ria F, Palu G, Fadda G, Manganelli R, Delogu G. 2010. Surface expression of MPT64 as a fusion with the PE domain of PE_PGRS33 enhances Mycobacterium bovis BCG protective activity against Mycobacterium tuberculosis in mice. Infect Immun 78:5202–5213. https://doi.org/10.1128/IAI.00267-10.
6. Clark SO, Delogu G, Rayner E, Sali M, Williams A, Manganelli R. 2015. Improved protection in guinea pigs after vaccination with a recombinant BCG expressing MPT64 on its surface. Trials Vaccinol 4:29–32. https://doi.org/10.1016/j.trivac.2015.03.003.
7. Nieuwenhuizen NE, Kaufmann SHE. 2018. Next-generation vaccines based on bacille Calmette-Guerin. Front Immunol 9:121. https://doi.org/10.3389/fimmu.2018.00121.
8. Nieuwenhuizen NE, Kulkarni PS, Shaligram U, Cotton MF, Rentsch CA, Eisele B, Grode L, Kaufmann SHE. 2017. The recombinant bacille Calmette-Guerin vaccine VPM1002: ready for clinical efficacy testing. Front Immunol 8:1147. https://doi.org/10.3389/fimmu.2017.01147.
9. Arbues A, Aguilo JI, Gonzalo-Asensio J, Marinova D, Uranga S, Puentes E, Fernandez C, Parra A, Cardona PJ, Vilaplana C, Ausina V, Williams A, Clark S, Malaga W, Guilhot C, Gicquel B, Martin C. 2013. Construction, characterization and preclinical evaluation of MTBVAC, the first live-attenuated M. tuberculosis-based vaccine to enter clinical trials. Vaccine 31:4867–4873. https://doi.org/10.1016/j.vaccine.2013.07.051.
10. Gonzalo-Asensio J, Marinova D, Martin C, Aguilo N. 2017. MTBVAC: attenuating the human pathogen of tuberculosis (TB) toward a promising vaccine against the TB epidemic. Front Immunol 8:1803. https://doi.org/10.3389/fimmu.2017.01803.
11. Hernandez Pando R, Aguilar LD, Smith I, Manganelli R. 2010. Immunogenicity and protection induced by a Mycobacterium tuberculosis sigE mutant in a BALB/c mouse model of progressive pulmonary tuberculosis. Infect Immun 78:3168–3176. https://doi.org/10.1128/IAI.00023-10.
12. Troudt J, Creissen E, Izzo L, Bielefeldt-Ohmann H, Casonato S, Manganelli R, Izzo AA. 2017. Mycobacterium tuberculosis sigE mutant ST28 used as a vaccine induces protective immunity in the guinea pig model. Tuberculosis (Edinb) 106:99–105. https://doi.org/10.1016/j.tube.2017.07.009.
13. Manganelli R. 2014. Sigma factors: key molecules in Mycobacterium tuberculosis physiology and virulence Microbiol Spectr 2:MGM2-0007-2013. https://doi.org/10.1128/microbiolspec.MGM2-0007-2013.
14. Manganelli R, Provvedi R. 2010. An integrated regulatory network including two positive feedback loops to modulate the activity of σ^E in mycobacteria. Mol Microbiol 75:538–542. https://doi.org/10.1111/j.1365-2958.2009.07009.x.
15. Boldrin F, Mazzabo LC, Anoosheh S, Palu G, Gaudreau L, Manganelli R, Provvedi R. 2019. Assessing the role of Rv1222 (RseA) as an anti-sigma factor of the Mycobacterium tuberculosis extracytoplasmic sigma factor SigE. Sci Rep 9:4513. https://doi.org/10.1038/s41598-019-41183-4.
16. Pisu D, Provvedi R, Espinosa DM, Payan JB, Boldrin F, Palu G, Hernandez-Pando R, Manganelli R. 2017. The alternative sigma factors SigE and SigB are involved in tolerance and persistence to antitubercular drugs. Antimicrob Agents Chemother 61:e01596-17. https://doi.org/10.1128/AAC.01596-17.
17. Manganelli R, Voskuil MI, Schoolnik GK, Smith I. 2001. The *Mycobacte-*

rium tuberculosis ECF sigma factor SigE: role in global gene expression and survival in macrophages. Mol Microbiol 41:423–437. https://doi.org/10.1046/j.1365-2958.2001.02525.x.
18. Manganelli R, Fattorini L, Tan D, Iona E, Orefici G, Altavilla G, Cusatelli P, Smith I. 2004. The extracytoplasmic function sigma factor SigE is essential for *Mycobacterium tuberculosis* virulence in mice. Infect Immun 72:3038–3041. https://doi.org/10.1128/iai.72.5.3038-3041.2004.
19. Manganelli R, Gennaro ML. 2017. Protecting from envelope stress: variations on the phage-shock-protein theme. Trends Microbiol 25:205–216. https://doi.org/10.1016/j.tim.2016.10.001.
20. Casonato S, Provvedi R, Dainese E, Palu G, Manganelli R. 2014. Mycobacterium tuberculosis requires the ECF sigma factor SigE to arrest phagosome maturation. PLoS One 9:e108893. https://doi.org/10.1371/journal.pone.0108893.
21. Walker KB, Brennan MJ, Ho MM, Eskola J, Thiry G, Sadoff J, Dobbelaer R, Grode L, Liu MA, Fruth U, Lambert PH. 2010. The second Geneva Consensus: recommendations for novel live TB vaccines. Vaccine 28:2259–2270. https://doi.org/10.1016/j.vaccine.2009.12.083.
22. Kamath AT, Fruth U, Brennan MJ, Dobbelaer R, Hubrechts P, Ho MM, Mayner RE, Thole J, Walker KB, Liu M, Lambert PH. 2005. New live mycobacterial vaccines: the Geneva consensus on essential steps towards clinical development. Vaccine 23:3753–3761. https://doi.org/10.1016/j.vaccine.2005.03.001.
23. Broset E, Martin C, Gonzalo-Asensio J. 2015. Evolutionary landscape of the Mycobacterium tuberculosis complex from the viewpoint of PhoPR: implications for virulence regulation and application to vaccine development. MBio 6:e01289-15. https://doi.org/10.1128/mBio.01289-15.
24. Hernandez-Pando R, Pavon L, Arriaga K, Orozco H, Madrid-Marina V, Rook G. 1997. Pathogenesis of tuberculosis in mice exposed to low and high doses of an environmental mycobacterial saprophyte before infection. Infect Immun 65:3317–3327.
25. Norouzi S, Aghamohammadi A, Mamishi S, Rosenzweig SD, Rezaei N. 2012. Bacillus Calmette-Guerin (BCG) complications associated with primary immunodeficiency diseases. J Infect 64:543–554. https://doi.org/10.1016/j.jinf.2012.03.012.
26. Marquina-Castillo B, Garcia-Garcia L, Ponce-de-Leon A, Jimenez-Corona ME, Bobadilla-Del Valle M, Cano-Arellano B, Canizales-Quintero S, Martinez-Gamboa A, Kato-Maeda M, Robertson B, Young D, Small P, Schoolnik G, Sifuentes-Osornio J, Hernandez-Pando R. 2009. Virulence, immunopathology and transmissibility of selected strains of Mycobacterium tuberculosis in a murine model. Immunology 128:123–133. https://doi.org/10.1111/j.1365-2567.2008.03004.x.
27. Lopez-Lopez N, Martinez AGR, Garcia-Hernandez MH, Hernandez-Pando R, Castaneda-Delgado JE, Lugo-Villarino G, Cougoule C, Neyrolles O, Rivas-Santiago B, Valtierra-Alvarado MA, Rubio-Caceres M, Enciso-Moreno JA, Serrano CJ. 2018. Type-2 diabetes alters the basal phenotype of human macrophages and diminishes their capacity to respond, internalise, and control Mycobacterium tuberculosis. Mem Inst Oswaldo Cruz 113:e170326. https://doi.org/10.1590/0074-02760170326.
28. Han SJ, Song T, Cho YJ, Kim JS, Choi SY, Bang HE, Chun J, Bai GH, Cho SN, Shin SJ. 2015. Complete genome sequence of Mycobacterium tuberculosis K from a Korean high school outbreak, belonging to the Beijing family. Stand Genomic Sci 10:78. https://doi.org/10.1186/s40793-015-0071-4.
29. Casadaban MJ, Cohen SN. 1980. Analysis of gene control signals by DNA fusion and cloning in Escherichia coli. J Mol Biol 138:179–207. https://doi.org/10.1016/0022-2836(80)90283-1.
30. Lefford MJ. 1978. Immunization of mice after airborne infection with various strains of BCG. Am Rev Respir Dis 117:103–109.
31. Gorak-Stolinska P, Weir RE, Floyd S, Lalor MK, Stenson S, Branson K, Blitz R, Luke S, Nazareth B, Ben-Smith A, Fine PE, Dockrell HM. 2006. Immunogenicity of Danish-SSI 1331 BCG vaccine in the UK: comparison with Glaxo-Evans 1077 BCG vaccine. Vaccine 24:5726–5733. https://doi.org/10.1016/j.vaccine.2006.04.037.
32. Bewick V, Cheek L, Ball J. 2004. Statistics review 12: survival analysis. Crit Care 8:389–394. https://doi.org/10.1186/cc2955.
33. James BW, Williams A, Marsh PD. 2000. The physiology and pathogenicity of Mycobacterium tuberculosis grown under controlled conditions in a defined medium. J Appl Microbiol 88:669–677. https://doi.org/10.1046/j.1365-2672.2000.01020.x.
34. Williams A, James BW, Bacon J, Hatch KA, Hatch GJ, Hall GA, Marsh PD. 2005. An assay to compare the infectivity of Mycobacterium tuberculosis isolates based on aerosol infection of guinea pigs and assessment of bacteriology. Tuberculosis (Edinb) 85:177–184. https://doi.org/10.1016/j.tube.2004.11.001.
35. Clark SO, Hall Y, Kelly DL, Hatch GJ, Williams A. 2011. Survival of Mycobacterium tuberculosis during experimental aerosolization and implications for aerosol challenge models. J Appl Microbiol 111:350–359. https://doi.org/10.1111/j.1365-2672.2011.05069.x.
36. Hartings JM, Roy CJ. 2004. The automated bioaerosol exposure system: preclinical platform development and a respiratory dosimetry application with nonhuman primates. J Pharmacol Toxicol Methods 49:39–55. https://doi.org/10.1016/j.vascn.2003.07.001.
37. Williams A, Hatch GJ, Clark SO, Gooch KE, Hatch KA, Hall GA, Huygen K, Ottenhoff TH, Franken KL, Andersen P, Doherty TM, Kaufmann SH, Grode L, Seiler P, Martin C, Gicquel B, Cole ST, Brodin P, Pym AS, Dalemans W, Cohen J, Lobet Y, Goonetilleke N, McShane H, Hill A, Parish T, Smith D, Stoker NG, Lowrie DB, Kallenius G, Svenson S, Pawlowski A, Blake K, Marsh PD. 2005. Evaluation of vaccines in the EU TB Vaccine Cluster using a guinea pig aerosol infection model of tuberculosis. Tuberculosis (Edinb) 85:29–38. https://doi.org/10.1016/j.tube.2004.09.009.